

Effects of Pressure on Volume-Recovery Experiments

Richard E. Robertson*

Research Staff, Ford Motor Company, Dearborn, Michigan 48121

Robert Simha†

Department of Macromolecular Science, Case Western Reserve University, Cleveland, Ohio 44106

John G. Curro‡

Sandia National Laboratories, Albuquerque, New Mexico 87185. Received June 11, 1985

ABSTRACT: Predictions are made for the following, based on our recent theory for volume recovery in polymer glasses: (1) volume recovery following a temperature step at constant pressure for various elevated pressures; (2) volume recovery following a pressure step at constant temperature; (3) volume recovery of densified glasses formed by compressing the liquid, cooling it below the glass transition temperature, and then releasing the pressure. The temperature at which the pressure is released is chosen so that the resulting total volume is equal to the equilibrium volume at that temperature and pressure (the volume obtained by extrapolating along the liquid line). The first two types of experiments were performed by Rehage and Goldbach on polystyrene, and the calculated results are compared with their experimental results.

Introduction

We have recently developed a kinetic theory for structural recovery or physical aging in the glassy state.¹⁻³ It is based on a stochastic model previously introduced by Robertson⁴⁻⁶ and makes use of Simha and Somcynsky's excess free volume function and its fluctuations, originally introduced for the equilibrium melt⁷ and subsequently extended to the quasi-equilibrium glass^{8,9} and finally to the relaxing glass.¹⁰ Expressions for the spectrum of retardation times and the time-dependent distribution of free volume were obtained, and the theory was successfully applied to the volume recovery, following temperature jumps at atmospheric pressure, as measured by Kovacs for poly(vinyl acetate).¹¹

The purpose of this paper is to explore the predictions of the theory for three types of volume-recovery experiments in which the pressure is different from, or is not maintained at, 1 bar. In the first, the temperature is stepped up or down at constant pressure for pressures exceeding 1 bar. In the second, the pressure is stepped at constant temperature. In the third, volume recovery is examined for densified glasses formed by compressing the liquid, cooling it below the glass transition temperature, and then releasing the pressure. Throughout, polystyrene is used as the example material. The third type of experiment has not been performed as such, but related experiments indicate that the final state after depressurizing is not in fact in equilibrium. We suggest that it differs from equilibrium by having a nonequilibrium free volume distribution. The changes in volume during volume recovery for different assumed free volume distributions are described.

Theory

The following is a summary of the theory, the details of which are given in ref 1. The changes in the measured volume associated with structural recovery are assumed to be due to changes in free volume. The free volume employed is the excess free volume given by the Simha-Somcynsky theory for the equation of state.⁷ The equation

of state given by the Simha-Somcynsky theory is

$$\bar{p}\bar{V}/\bar{T} = [1 - y(2^{1/2}y\bar{V})^{-1/3}]^{-1} + (y/\bar{T})[2.022(y\bar{V})^{-4} - 2.409(y\bar{V})^{-2}] \quad (1)$$

where \bar{p} , \bar{V} , and \bar{T} are the reduced variables, $\bar{p} = p/p^*$, $\bar{V} = V/V^*$, and $\bar{T} = T/T^*$, with p^* , V^* , and T^* being the characteristic scaling parameters for each polymer material, and y is the fractional occupancy of the cells. The free volume, or fractional free volume, is defined by

$$f = 1 - y \quad (2)$$

At equilibrium, the free volume or occupancy is determined by the minimization of the free energy. This minimization yields

$$(s/3c)[(s-1)/s + y^{-1} \ln(1-y)] = [y(2^{1/2}y\bar{V})^{-1/3} - 1/3]/[1 - y(2^{1/2}y\bar{V})^{-1/3}] + (y/6\bar{T})[2.409(y\bar{V})^{-2} - 3.033(y\bar{V})^{-4}] \quad (3)$$

where s is the degree of polymerization of the polymer and c is a measure of the degrees of freedom of the polymer and will be assumed to be such that $s/3c = 1$. When the polymer is not at equilibrium, eq 3 is not valid, and a different condition is needed to reduce the number of variables in eq 1. Sometimes the volume V can be estimated or determined by experiment. For example, when the temperature or pressure of the polymer is suddenly stepped to a new value, the polymer behaves like a glass, and the volume changes accordingly. The new volume is easily estimated, and eq 1 is used to determine the free volume f . On the other hand, during structural recovery, the dynamical theory of the free volume described below can yield the time-dependent free volume f . Then, it is the volume V that is computed from eq 1.

To compute the changes in free volume during recovery, it is necessary to examine changes occurring locally throughout the entire specimen. Local changes occur at rates that depend on the local free volume, which can vary from point to point because of thermal fluctuations. At equilibrium, the mean squared thermal fluctuation in free volume, $\langle \delta f^2 \rangle$, which equals the mean squared thermal fluctuations in cell occupancy, $\langle \delta y^2 \rangle$, is given approximately by¹

* Supported by NSF Grant DMR-84-08341.

† Supported by U.S. DOE DE-AC04-76 DP00789.

$$N_s \langle \delta f^2 \rangle = \left\{ \left[1 + (2/y) \ln(1-y) + 1/(1-y) \right] / y^2 + \frac{1}{3} \frac{(2^{1/2} y \tilde{V})^{2/3} - (8/3) y (2^{1/2} y \tilde{V})^{1/3} + 3y^2}{y^2 [2^{1/2} y \tilde{V}^{1/3} - y]^2} + \frac{1}{3y \tilde{T}} [6.066(y \tilde{V})^{-4} - 2.409(y \tilde{V})^{-2}] \right\}^{-1} \quad (4)$$

where N_s represents the size of the regions of interest and is the nominal number of monomers in those regions.

The value usually assumed for N_s is the number of monomers estimated to be involved in local segmental rearrangements. For vinyl-type polymers, a chain segment of roughly four backbone carbon atoms or two monomer units plus twelve nearest neighbors of like size is expected to constitute a segmental rearrangement cell.¹² This would yield $N_s = 26$ monomers. Different values of N_s may be appropriate for other polymers. Also, problems with the numerical solution sometimes require further changes of N_s . For these reasons, N_s is treated as an adjustable parameter in the computation.

Although eq 4, like eq 1, is derived under the general assumption of equilibrium, the specific assumption of the minimization of the free energy has not been made. Hence, under conditions where the free volume distribution has properties, including shape, similar to those existing at equilibrium, eq 4 still can be used as an approximation. This is expected to be so for the glass formed from an equilibrium liquid by the sudden (instantaneous) change in temperature or pressure.

Although the fractional free volume existing within the regions of interest, the segmental rearrangement cells, represents a continuous distribution, the computation of the changes of free volume within these cells is more easily performed if the distribution is discrete. Thus, the N_s monomer-size cells are assumed to contain only certain well-defined amounts of free volume, which are assumed to be multiples of a quantity denoted by β . These discrete amounts of free volume therefore represent a set of "free volume states".

The fraction of cells that have at time t the free volume $(j-1)\beta$ will be denoted by $w_j(t)$. The index j , which describes the set of free volume states, runs from 1 to n . The upper limit n is set high enough that almost no regions would have a free volume greater than $(n-1)\beta$. The computation of the changes in free volume during a structural recovery involves computing the changes in the free volume distribution or the w_j 's with time.

At equilibrium, the free volume distribution is expected to be nearly Gaussian, except that the free volume cannot assume negative values. A discrete distribution function that can reflect this behavior is the binomial distribution. The binomial distribution has two parameters: the number of states n and the unit probability p_r . The unit probability p_r and the free volume increment β are fixed by demanding that the binomial distribution yield the correct mean and variance:

$$\begin{aligned} (n-1)p_r\beta &= \langle f \rangle \\ (n-1)p_r(1-p_r)\beta^2 &= \langle \delta f^2 \rangle \end{aligned} \quad (5)$$

The state occupancies given by the binomial distribution are

$$\xi_j = \binom{n-1}{j-1} p_r^{j-1} (1-p_r)^{n-j} \quad (6)$$

For an equilibrium state, or approximately for the state resulting from a sudden step in temperature or pressure applied to an equilibrium state, we have $w_j = \xi_j$.

The transitions among the various free volume states since an earlier time t_0 represent a stochastic process, depending on Brownian motion, and can be described formally by the following set of n equations:¹³

$$w_j(t) = \sum_{i=1}^n w_i(t_0) P_{ij}(t-t_0) \quad (7)$$

where $P_{ij}(t-t_0)$ is the transition probability from states i to j during the time interval from t_0 to t . Notice that the probability of a transition out of a state i is assumed proportional to the occupancy of state i . If the transitions between any pair of states are assumed to pass through all of the intervening states, then over an infinitesimal time interval h , the transition probabilities for a state i become, approximately,

$$\begin{aligned} P_{i,i-1}(h) &= h\lambda_i^- \\ P_{i,i+1}(h) &= h\lambda_i^+ \\ P_{ii}(h) &= 1 - h(\lambda_i^- + \lambda_i^+) \end{aligned} \quad (8)$$

with all the other P_{ij} 's approximately equal to zero, where λ_i^+ and λ_i^- are the upward and downward transition rates from state i , respectively. Because the transition probabilities behave according to the following equation¹³

$$P_{ij}(t+h) = \sum_{k=1}^n P_{ik}(t) P_{kj}(h) \quad (9)$$

the time derivative of this equation with respect to h yields a set of coupled differential equations, which can be written in matrix form as

$$\dot{\mathbf{P}}(t) = \mathbf{P}(t) \cdot \mathbf{A} \quad (10)$$

where \mathbf{A} is a tridiagonal matrix with $A_{ii} = -(\lambda_i^- + \lambda_i^+)$, $A_{i,i-1} = \lambda_i^-$ and $A_{i,i+1} = \lambda_i^+$ (except for $i=1$ and n , where transitions outside the range of i are not allowed).

The upward and downward transition rates are not independent but are linked at equilibrium by the requirements of detailed balancing:

$$\xi_i \lambda_i^+ = \xi_{i+1} \lambda_{i+1}^- \quad (11)$$

The transition rates are expected to depend on the local free volume. Thus, the transition rate out of state i will be a function of the free volume $(i-1)\beta$, for example. In addition, the rates are expected to depend on the free volume of the immediately adjacent region. This is because the surrounding region must act as the source and sink for changes in free volume. The form of the volume dependence in the statistical mechanical equation for fluctuations indicates that there is no correlation between fluctuations in neighboring regions. As a result, the free volume averaged over the roughly 12 N_s -size regions that make up the surrounding region will be nearly equal to the global average, $\langle f \rangle$, and will be independent of the free volume of the central region. The free volume affecting the transition rates out of a state i can then be described by¹

$$\hat{f}_i = [(i-1)\beta + (z-1)\langle f \rangle] / z \quad (12)$$

where $(z-1)$ is the number of N_s monomer-size regions acting as the local environment to liberate or absorb free volume. Since the environment consists essentially of the nearest neighbors, z has roughly the value of 13. But like N_s , the value for z is treated as an adjustable parameter in the computation. (For the sensitivity of N_s and z , see Figures 11 and 12 of ref 1.)

The local transition rates are assumed to depend on the local free volume in the same way that the global kinetics depend on the global free volume. For this purpose, we express the WLF (Williams-Landel-Ferry) or the Vogel equation in terms of free volume instead of temperature. Because of the near linearity between f , the free volume given by the Simha-Somcynsky equation, and temperature, the following substitution is made in the WLF and Vogel equations:

$$T - T_g = (f - f_g)T^*/f^* \quad (13)$$

where f^* , a "characteristic free volume" defined by this equation, is obtained from plots of the free volume of the liquid above the glass temperature vs. temperature at constant pressure. Note that this substitution in the empirically derived WLF and Vogel equations involves no assumptions other than that there exists this one-to-one correspondence between T and f in the equilibrium liquid state. The assumption to be made, however, is that the WLF and Vogel equations, when expressed in terms of free volume instead of temperature, can be used to represent local transition rates when the system is away from global equilibrium.

With the Vogel form of the rate equation, the rate for the downward step in local free volume is written as

$$\lambda_i^- = R\tau_g^{-1}(\xi_{i-1}/\xi_i)^{1/2}\beta^{-2} \exp\{2.303c_1[1 + c_2/(c_2 + T^*(\hat{f}_i - f_g)/f^*)]\} \quad (14)$$

where R is an adjustable constant that acts to translate from microscopic to macroscopic processes and τ_g is the relaxation time at the glass transition. R is used also to compensate for inexact or uncertain values of τ_g . The rate for the upward step is given by eq 11 along with eq 14. The factor $(\xi_{i-1}/\xi_i)^{1/2}$ in eq 14 gives the same form to the rates for the upward and downward steps, and the factor β^{-2} removes the free volume step size from the overall kinetics.

The formal solution to the differential equation in eq 10 is

$$\mathbf{P}(t) = \mathbf{P}(0) \exp(\mathbf{A}t) \quad (15)$$

To obtain a more explicit form for the solution, the eigenvalues of \mathbf{A} need to be found. It is convenient to first symmetrize \mathbf{A} . By applying a similarity transformation with a diagonal matrix γ , the symmetrical matrix $\mathbf{Z} = \gamma^{-1}\mathbf{A}\gamma$ is obtained, where

$$\gamma_i = \xi_i^{-1/2} \quad (16)$$

Then, in terms of the eigenvalues ξ_k and the corresponding eigenvectors \mathbf{Q}_k of the matrix \mathbf{Z} , the free volume state populations develop in time according to

$$w_i(t) = \sum_{k=1}^n \gamma_i^{-1} Q_{ik} \left[\sum_{j=1}^n w_j(t_0) \gamma_j Q_{jk} \right] \exp[\xi_k(t - t_0)] \quad (17)$$

Because the eigenvalues ξ_k for $k = 1, \dots, n$ are all negative, the right-hand side of eq 17 is equivalent to a sum of decaying exponentials. But the changes in the populations w_i are not quite describable by a parallel array of Maxwell models, say. Because of the dependence given in eq 12 of \hat{f}_i on the average free volume, which changes continuously during recovery, the values of the parameters in eq 17 have to be continually reevaluated. Hence, the relaxation has features of what Palmer et al. have called a series of type of relaxation.¹⁴

The average free volume is given by

$$\langle f(t) \rangle = \sum_{j=2}^n (j-1)\beta w_j(t) \quad (18)$$

Table I
Parameters for Recovery Kinetics of Polystyrene

$p^* = 7453 \text{ bar}^a$	Simha-Somcynsky characteristic parameters
$a^* = 0.9598 \text{ cm}^3/\text{g}^a$	
$T^* = 12680 \text{ K}^a$	
$c_1 = 13.3^b$	time-temperature shift parameters
$c_2 = 47.5 \text{ K}^b$	
$T_g = 373 \text{ K}$	
$\tau_g = 1 \text{ h (3600 s)}$	nominal relaxation time at glass transition
$N_g = 40$	
$z = 12$	
$R = 5.3$	
	no. of segments in free volume region
	size ratio for region controlling free volume
	translation factor between macroscopic and microscopic processes

^aQuach, A.; Simha, R. *J. Appl. Phys.*, 1971, 42, 4592. ^bPlazek, D. J. *J. Phys. Chem.* 1965, 69, 3480.

The changes in volume, $V(t)$, during structural recovery or physical aging are found from eq 1 with $y = 1 - \langle f(t) \rangle$.

Determination of Parameters

To compute the recovery kinetics of polystyrene under different histories of pressure and temperature, a number of material parameters are needed. Some of these are given in Table I for polystyrene. The first three quantities in Table I are the Simha-Somcynsky characteristic parameters for the pressure-volume-temperature properties of the liquid. All of the desired p - V - T properties and the free volume functions for the liquid can be derived from the Simha-Somcynsky theory with these parameters. For the glass, however, certain parameters need to be obtained from experiment. These include the glass transition temperature itself, as a function of pressure, $T_g(p)$, the thermal expansivity of the glass as a function of pressure, α_{glass} , and the compressibility or bulk modulus of the glass as a function of temperature and pressure, B_{glass} . Further quantities are the time-temperature shift parameter of the liquid as a function of temperature and pressure, $a_{T,p}$, and the transition region size parameters N_g and z . The evaluation of these is discussed in the Appendix. Ideally, each of the parameters should be determined for the same polymer specimen. Unfortunately, this has not been possible with polystyrene.

Volume Recovery from Temperature Steps under Constant Pressure

The computation of volume recovery following temperature steps under constant pressure for polystyrene is analogous to that described earlier for poly(vinyl acetate).¹ The polymer is assumed to be in equilibrium at the initial temperature T_0 , and then at time $t = 0$, the temperature is suddenly stepped to the final temperature T_1 . Rehage and Goldbach^{15,16} have measured the volume recovery following temperature steps at 1-bar pressure for polystyrene. The data are shown in Figure 1 for steps from various initial temperatures, T_0 , to the final temperature, T_1 , of 90.70 °C. The polystyrene had been thermally polymerized and had a number-average molecular weight of 500 000. The ordinate in Figure 1 is the relative deviation of the volume from equilibrium; the volume difference in the denominator, $(V_0 - V_1)$, is that existing immediately after the step in temperature. The computed curves, given by the solid lines, were moved along the time axis until a reasonable fit with the data was obtained. The fit to the data in Figure 1 is fairly good and yields the parameter of R in Table I. (The large difference between the value of R for polystyrene (5.3) and that used previously for poly(vinyl acetate) (0.0022) is believed to arise largely from different relaxation times at the assumed glass transition temperatures. Although τ_g was set equal to 1 h for both, the actual relaxation times are unknown.)

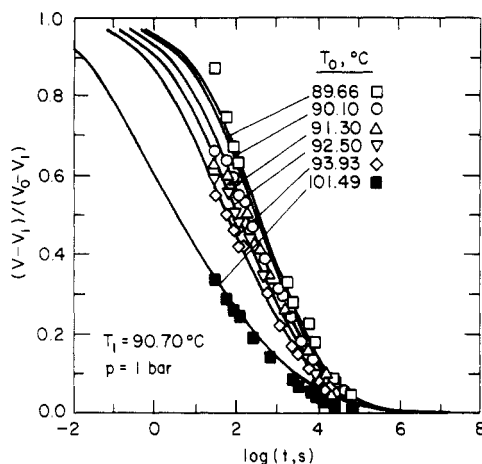


Figure 1. Experimental and computed volume recovery vs. time of polystyrene from temperature steps of various magnitude to 90.70 °C at 1-bar pressure. Data from Rehage and Goldbach.^{15,16}

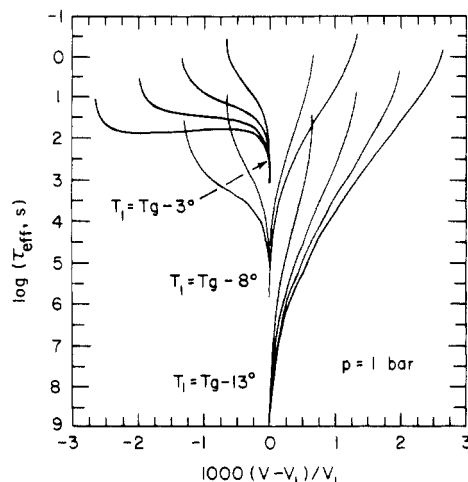


Figure 2. Effective relaxation times vs. deviation from equilibrium computed for volume recovery of polystyrene from temperature steps at 1-bar pressure. All combinations of steps from $T_0 = 360, 362.5, 365, 367.5$, and 370 K to $T_1 = 360, 365$, and 370 K are shown. ($T_g = 373$ K.)

Rehage and Goldbach's volume recovery from temperature steps data for polystyrene have been fitted because they are the companion to volume-recovery data from pressure steps, to be described in the next section. The results basically agree with those of Kovacs,¹⁷ Hozumi, Wakabayashi, and Sugihara,¹⁸ Uchidoi, Adachi, and Ishida,¹⁹ and Adachi and Kotaka.²⁰

Using the parameters for polystyrene mentioned above, including the value of R derived from the fit in Figure 1, predictions for other volume-recovery experiments can be made. Figures 2 and 3 show the effective relaxation times computed for volume recovery vs. the relative deviation of the volume from equilibrium following temperature steps under the pressures of 1 bar and 1 kbar, respectively. The effective relaxation time is related to the instantaneous volume V by

$$\tau_{\text{eff}}^{-1} = -(dV/dt)(V - V_{\text{eq}})^{-1} \quad (19)$$

where V_{eq} is the equilibrium volume. These curves are analogous to those first presented by Kovacs for poly(vinyl acetate).¹¹ These plots contain the same information as plots of V vs. time and are somewhat more sensitive to changes in V with time.

Twelve different temperature step experiments from T_0 to T_1 are represented in each of Figures 2 and 3. The initial temperatures (T_0) were $T_g - 13$ °C, $T_g - 10.5$ °C, T_g

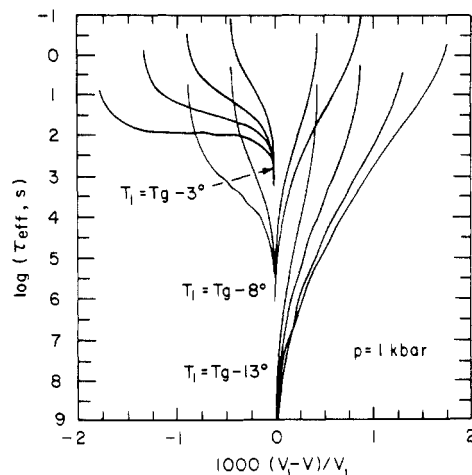


Figure 3. Effective relaxation times vs. deviation from equilibrium computed for volume recovery of polystyrene from temperature steps at 1-kbar pressure. All combinations of steps from $T_0 = 389.4, 391.9, 394.4, 396.9$, and 399.4 K to $T_1 = 389.4, 394.4$, and 399.4 K are shown. ($T_g = 402.4$ K.)

-8 °C, $T_g - 5.5$ °C, and $T_g - 3$ °C. The final temperatures (T_1) were $T_g - 13$ °C, $T_g - 8$ °C, and $T_g - 3$ °C. ($T_g = 373$ K at 1 bar, and $T_g = 402.4$ K at 1 kbar.) All combinations of these initial and final temperatures are represented in Figures 2 and 3. The computation begins immediately after the step.

Overall, the curves in Figures 2 and 3 appear similar to those previously computed for poly(vinyl acetate).¹ N_s and z were chosen so that this would occur, however. (A certain amount of "ripple" is visible in these curves. This is due to a diagonalization problem mentioned in the Appendix in connection with the choice of N_s and z . The ripple is considerably exacerbated for polystyrene when $N_s = 26$ and $z = 13$, as they were for poly(vinyl acetate).) In addition, for the same temperature step relative to T_g , the isothermal kinetics of volume recovery appears not to be appreciably affected by increasing the pressure from 1 bar to 1 kbar. The main difference between the curves for polystyrene in Figures 2 and 3 and those for poly(vinyl acetate) is that the volume changes by a smaller amount for polystyrene for a given change in temperature, which makes accurate measurements of volume more important. This is even more true as the pressure is increased. The initial deviation in volume at 1 kbar is only two-thirds that at 1 bar, for the same temperature difference.

Volume Recovery from Pressure Steps at Constant Temperature

The computation of volume recovery following pressure steps at constant temperature is analogous to that described above for temperature steps under constant pressure. The polymer is assumed to be in equilibrium at the initial pressure p_0 and temperature T . Then at time $t = 0$, the pressure is suddenly stepped to the final value p_1 without change in temperature. Rehage and Goldbach^{15,16} have measured the volume recovery following pressure steps from several elevated pressures down to atmospheric pressure at the temperature of 91.84 °C. Their data are shown in Figure 4 along with the computed predictions. The parameters in the computation were the same as those used for the volume recovery following temperature steps discussed in the preceding section, including the value of R obtained from fitting those data.

The fit between experiment and computation in Figure 4 is approximate. One important feature reproduced in the calculation is the degree of spread between the curves in the two figures, Figures 1 and 4. Rehage and Goldbach

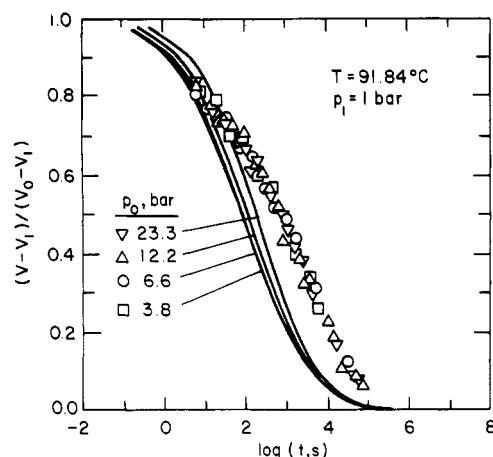


Figure 4. Experimental and computed volume recovery vs. time of polystyrene from pressure steps of various magnitude to 1 bar at 91.84 °C. Data from Rehage and Goldbach.^{15,16}

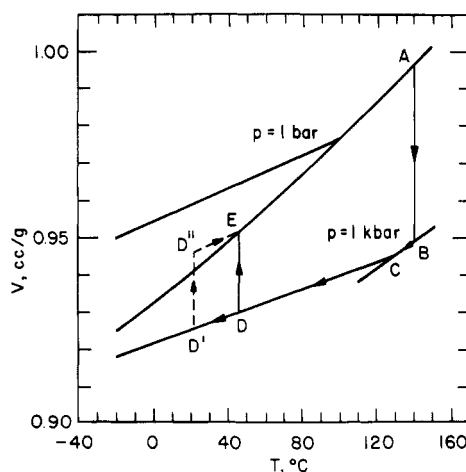


Figure 5. Paths for attaining equilibrium volume below the glass transition temperature at atmospheric pressure with densified glass.

drew particular attention to the much larger spread in the temperature-step than in the pressure-step data. This difference is predicted also by the theory. However, it is presently unclear why there is not better agreement between theory and experiment. In contrast to the assumptions of the computation, the data seem to suggest that recovery from pressure steps is basically different from recovery from temperature steps. Although the recovery from the pressure steps occurred at a higher temperature than the recovery from the temperature steps, the former is relatively slower. Lacking the usual S-shape slowdown as equilibrium is reached, however, the recovery from the pressure steps appears to be complete at nearly the same time as that from the temperature steps. Because of experimental difficulties, such a detailed comparison of the data may be inappropriate, however.

Volume Recovery in Densified Glasses

Densified glasses allow further exhibition of structural recovery or physical aging. For instance, one can consider the following question: Is it possible to rapidly reach an equilibrium liquid state below the glass transition temperature at atmospheric pressure by pressurizing the liquid, cooling it below the glass transition, and then depressurizing it? This sequence of steps is shown schematically in Figure 5. The liquid at A is pressurized to B, cooled through the glass transition at C to D, and then depressurized to E, the equilibrium volume at atmospheric

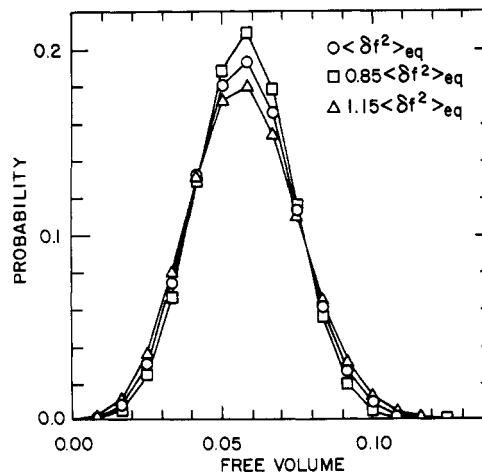


Figure 6. Free volume distribution in polystyrene at 90 °C at equilibrium (O) and for the mean squared fluctuation, $\langle \delta f^2 \rangle$, 15% smaller (□) and 15% larger (Δ) than equilibrium.

pressure at that temperature. An alternative path, indicated by the dashed line, would be to cool the pressurized glass to room temperature at D' before releasing the pressure and then heating the depressurized glass from D' to E. It would seem that for either path, the equilibrium volume at E would be more quickly reached in this way than if the glass had been cooled at atmospheric pressure to the temperature of E and allowed to recover to E.

Although the densified glass at E in Figure 5 has the equilibrium volume, is it in equilibrium? Various indirect experiments suggest that it is not. For example, Oels and Rehage²³ found that all their densified glasses, produced under pressures up to 5000 bar, tended at 22 °C to expand with time. Yet one of these densified glasses had a volume very close to equilibrium at 22 °C immediately following depressurization, and so its volume would not have been expected to have changed, and glasses produced under lower pressure would have had volumes already larger than their equilibrium volumes following depressurization.

If the densified glass at E in Figure 5 has the equilibrium volume but is not in equilibrium, how is the nonequilibrium nature of this state to be described? The parameters other than volume used by the kinetic theory to describe the structure of the glass are the average free volume and the free volume distribution. Though it is possible that the average free volume of the state brought to E in this way is not the equilibrium value, it is in the nature of free volume, as it arises from the division of the total volume into filled and unfilled space, to assume that the average free volume will be in equilibrium whenever the total volume is. Therefore, in the following only the free volume distribution will be assumed not to be in equilibrium on arrival at E. There is still the question of whether the distribution has the symmetry of the equilibrium distribution. Since the average free volume has been assumed to be the equilibrium value at E in Figure 5, the free volume distribution is likely to be symmetrical at E as well.

The equilibrium free volume distribution at 90 °C for polystyrene for 40 monomer-size regions is shown in Figure 6. Also shown are the free volume distributions at 90 °C for distributions having mean squared fluctuations smaller and larger by 15% than at equilibrium. These distributions are roughly 8% narrower and broader, respectively, than the equilibrium distribution. The time developments of the volume for these distributions are shown in Figures 7 and 8.

If maintained at 90 °C, the densified glass with the narrower than equilibrium free volume distribution is seen

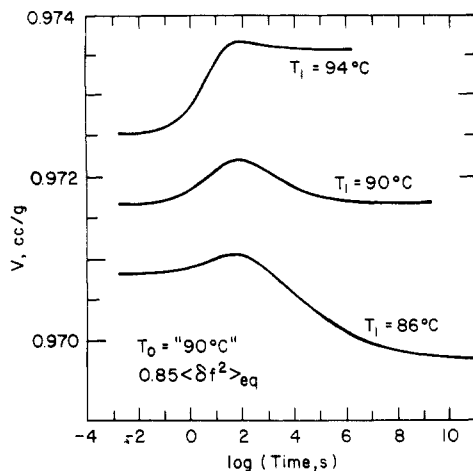


Figure 7. Development of the volume in time at 86, 90, and 94 °C for a glass having the equilibrium volume and free volume at 90 °C and a mean squared fluctuation in free volume 15% smaller than equilibrium.

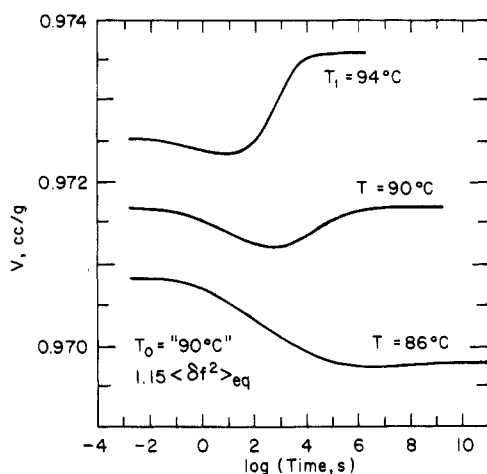


Figure 8. Development of the volume in time at 86, 90, and 94 °C for a glass having the equilibrium volume and free volume at 90 °C and a mean squared fluctuation in free volume 15% larger than equilibrium.

in Figure 7 to go through a maximum before returning to the initial (and equilibrium) volume. The reason for the maximum is that the higher free volume half of the distribution in Figure 6 moves up toward the upper half of the equilibrium distribution before the lower free volume half moves down. This causes the average free volume to go through a maximum, and, hence, so does the total volume. Later on, the lower half of the initial distribution will move downward to bring the distribution into equilibrium. In contrast, the densified glass with the broader free volume in Figure 6 is seen in Figure 8 to go through a minimum. This occurs in like manner because the upper half of the initial distribution moves downward toward the equilibrium distribution before the lower half of the initial distribution moves upward. An equilibrium distribution, of course, would not have changed.

In the computation of the volume-recovery curves in Figures 7 and 8, only thermal agitation or Brownian motion was assumed as the driving force for recovery. Stress field effects were not taken into account. Densified glasses immediately after the release of pressure, however, should be viewed as being under a negative pressure, because the release of pressure is tantamount to superimposing on the original pressure a negative pressure of equal magnitude. The distortions in the molecular geometry induced by packing at the elevated pressure represent a stable me-

chanical system at that pressure. But when the pressure is suddenly released, the distortions immediately revert back to those characteristic of lower pressure, and this acts effectively as an externally applied negative pressure, which is a further driving force for the expansion of the glass. Because this driving force was not included in the computation, higher temperatures, near the glass transition temperature, were needed to simulate the recovery that occurs rapidly at lower temperatures.

Since the densified glass may not be maintained at exactly the temperature at which its volume has the equilibrium value, the time development of the volume at temperatures both higher and lower than that also are shown in Figures 7 and 8. (The initial displacements of these curves upward and downward from the curves for 90 °C are due to the thermal expansion of the glass.) If the free volume distribution of the densified glass is narrower than equilibrium, a maximum is superimposed on the volume curve at the beginning or the end of the transition, whichever is at the higher volume. But the height of the maximum decreases as the temperature differs from that at which the volume was initially in equilibrium. If the free volume distribution of the densified glass is broader than equilibrium, a minimum is superimposed on the volume curve at the beginning or the end of the transition, whichever has the smaller volume. Note, however, that the minimum is not very distinct for the downstep to 86 °C in Figure 8. Although it seems possible for densified glasses to have free volume distributions that are either narrower or broader than equilibrium, densified polystyrene seems to have a narrower free volume distribution.^{21,22}

Acknowledgment. We appreciate the careful reading of the manuscript and helpful suggestions of Professor John J. Aklonis.

Appendix

Glass Transition Temperature. The glass transition temperature, $T_g(p)$, has been found to increase with pressure in all polymers for which it has been studied. Oels and Rehage²³ measured the transition for polystyrene over the pressure range of 1 to nearly 4000 bar. Their data can be represented by the equation

$$T_g(p) = 363.0 + 31.1 \times 10^{-3}p - 1.71 \times 10^{-6}p^2 \quad (\text{A1})$$

where the units of $T_g(p)$ are K and the units of p are bar. The temperature referred to in eq 1 is the point at which on cooling the glass transition is complete. In those instances where a different point in the transition is needed, eq 1 will be used except that the temperature of that point at zero pressure (usually 373 K) will replace the first term on the right-hand side.

Thermal Expansivity of the Glass. The thermal expansivity of the glass decreases slowly with increasing pressure. From their p - V - T measurements of polystyrene over a pressure range up to 4000 bar, Oels and Rehage²³ obtained a curve for the thermal expansivity that can be represented by

$$\alpha_{\text{glass}} = 2.24 \times 10^{-4} - 3.71 \times 10^{-8}p + 3.61 \times 10^{-12}p^2 \quad (\text{A2})$$

where the units of α_{glass} are $\text{cm}^3/\text{g K}$ and the units of p are bar. Because the changes in volume with temperature remains fairly linear with increasing pressure, α_{glass} suffices for our purposes to describe the change in volume with temperature.

Bulk Modulus of the Glass. The bulk modulus, the reciprocal of the isothermal compressibility, tends to in-

crease with decreasing temperature and increasing pressure. On the basis of curves given by Rehage²⁴ for atactic polystyrene, the bulk modulus may be represented by

$$B_{\text{glass}} = -5.766 \times 10^5 + 2902T - 3.30T^2 + (0.0212T - 0.85)p \quad (\text{A3})$$

where the units of B_{glass} are bar g/cm³, the units of T are K, and the units of p are bar.

Time-Temperature-Pressure Shift Parameter. According to Fillers, Moonan, and Tschoegl^{25,26} the time-temperature-pressure shift parameter, $a_{T,p}$, has the form

$$\log a_{T,p} = -c_1 + c_1 c_2(p) / [c_2(p) + T - T_0 - \theta(p)] \quad (\text{A4})$$

where c_2 and θ are functions of pressure only, T_0 is a fixed reference temperature, and c_1 is a constant, independent of both temperature and pressure. A convenient reference temperature is T_g at 1-bar pressure. At this temperature and pressure, $a_{T,p} = 1$. Because the liquid has essentially the same viscosity along the glass transition curve, $a_{T,p}$ remains constant and equal to 1 along this curve. Hence, one deduces that $T_0 + \theta(p) = T_g(p)$. To obtain $c_2(p)$, another relationship between temperature, pressure, and viscosity is needed. Cogswell and McGowan²⁷ measured viscosities in the range 10^4 – 10^6 N s/m² of a number of polymer liquids including polystyrene at pressures ranging up to 175 MPa (1750 bar). Unfortunately, because c_2 is a second-order term, its pressure dependence was not discernible from Cogswell and McGowan's data. Nor was the dependence discernible using the empirical viscosity equation derived by Cogswell and McGowan. Because currently available data are not able to indicate the pressure dependence of c_2 , it has been left independent of pressure in the calculations to follow.

The time-temperature-pressure shift parameter used for polystyrene, therefore, had the form

$$\log a_{T,p} = -c_1 + c_1 c_2 / [c_2 + T - T_g(p)] \quad (\text{A5})$$

But some uncertainty remains as to what values to use for c_1 and c_2 . Probably the best measurements of the time-temperature shift parameters for polystyrene are those by Plazek and O'Rourke^{28,29} on narrow molecular weight fractions. However, the recoverable shear compliance and the viscosity give different time-temperature shift parameters for these fractions.

There may be some similarity with poly(vinyl acetate), for which Plazek³⁰ found two adjacent transitions. The lower or "softening" transition region of poly(vinyl acetate) was exhibited by the recoverable shear compliance alone, whereas the upper or "terminal" transition region was exhibited by viscosity as well as by the recoverable shear compliance. For temperatures in the vicinity of the glass transition, the more appropriate time-temperature shift parameter was that from the softening region. For temperatures just above the glass transition, the softening time-temperature shift parameter described the volume recovery of poly(vinyl acetate) very well.³ But for temperatures below the glass transition, volume recovery was badly fitted by this time-temperature shift parameter, largely because it extrapolates below the glass transition to segmental mobilities that are too small. On the other hand, because the time-temperature shift parameter for the "terminal" region extrapolates to higher segmental mobilities below the glass transition, it was found to give a fair overall fit to volume-recovery data, although nowhere was the fit good. With a sufficient volume recovery for poly(vinyl acetate), the proper time-temperature shift parameter was deduced to be that from the softening re-

gion at temperatures above the glass temperature and a modified shift parameter below the glass transition.³ The modification of the shift parameter below the glass transition was suggested to arise from the contribution of the segmental mobilities associated with lower temperature loss peaks.

In analogy with poly(vinyl acetate), the more appropriate time-temperature shift parameter for the volume recovery of polystyrene above the glass transition is likely to be that from the recoverable shear compliance. But below the glass transition, this may give poor predictions of volume recovery. As a compromise, therefore, the constant values for c_1 and c_2 used and given in Table I are those derived from the viscosity. These were taken from Plazek's measurements on a narrow fraction having a molecular weight of 46 900.²⁸ The reference temperature is that of the glass transition. But because these values will be used to describe polystyrenes of higher molecular weight, the glass transition temperature of 373 K will be used, rather than the 370.7 K appropriate to the molecular weight of 47 000. Although the prediction of the volume recovery of polystyrene is not expected to be good in detail, the overall prediction is expected to be fair.

The nominal relaxation time at the glass transition temperature, τ_g , was set equal to 1 h. Discrepancies between this and the actual relaxation time at T_g was absorbed in the value of R , which multiplies τ_g in eq 14.

Transition Region Size Parameters. Two other required material parameters, which are included in Table I, are N_s and z . The values assigned to these parameters for poly(vinyl acetate) were 26 and 13, respectively.¹ To obtain the same qualitative behavior with polystyrene as with poly(vinyl acetate), it was necessary to change these values to those in Table I, viz., 40 and 12. The change was more of computational convenience than of substance. As was described previously,¹ N_s and z have nearly inverse effects on the computation, except close to equilibrium, and the increase of N_s and the decrease of z tend to cancel. But the change allows a definite trend to be established in the ranking of eigenvalues obtained from numerically diagonalizing the matrix A or Z in eq 15. Otherwise, the diagonalizing program EISPACK tends to misassign eigenvectors to eigenvalues because of a misranking of eigenvalues due to roundoff error. The reason that the problem is more prominent with polystyrene than with poly(vinyl acetate) seems to be related to the narrower free volume distribution and fewer discrete free volume states of significant occupation with polystyrene.

Registry No. Polystyrene (homopolymer), 9003-53-6.

References and Notes

- (1) Robertson, R. E.; Simha, R.; Curro, J. G. *Macromolecules* **1984**, *17*, 911.
- (2) Simha, R.; Curro, J. G.; Robertson, R. E. *Polym. Eng. Sci.* **1984**, *24*, 1071.
- (3) Robertson, R. E. *Macromolecules* **1985**, *18*, 953.
- (4) Robertson, R. E. *J. Polym. Sci., Polym. Symp.* **1978**, No. 63, 173.
- (5) Robertson, R. E. *J. Polym. Sci., Polym. Phys. Ed.* **1979**, *17*, 597.
- (6) Robertson, R. E. *Ann. N.Y. Acad. Sci.* **1981**, *371*, 21.
- (7) Simha, R.; Somcynsky, T. *Macromolecules* **1969**, *2*, 342.
- (8) Simha, R.; Wilson, P. S. *Macromolecules* **1973**, *6*, 908.
- (9) McKinnney, J. E.; Simha, R. *Macromolecules* **1976**, *9*, 430.
- (10) Curro, J. G.; Lagasse, R. R.; Simha, R. *Macromolecules* **1982**, *15*, 1621.
- (11) Kovacs, A. J. *Fortsch. Hochpolym. Forsch.* **1963**, *3*, 394.
- (12) Jelinski, L. W.; Dumais, J. J.; Engel, A. K. *Macromolecules* **1983**, *16*, 492.
- (13) van Kampen, N. G. "Stochastic Processes in Physics and Chemistry"; North-Holland Publishing Co.: Amsterdam, 1981.
- (14) Palmer, R. G.; Stein, D. L.; Abrahams, E.; Anderson, P. W. *Phys. Rev. Lett.* **1984**, *53*, 958.

- (15) Rehage, G.; Goldbach, G. *Ber. Bunsenges. Phys. Chem.* **1966**, *70*, 1144.
- (16) Goldbach, G.; Rehage, G. *J. Polym. Sci., Part C* **1967**, *16*, 2289.
- (17) Kovacs, A. J. *J. Polym. Sci.* **1958**, *30*, 131.
- (18) Hozumi, S.; Wakabayashi, T.; Sugihara, S. *Polym. J.* **1970**, *1*, 632.
- (19) Uchidoi, M.; Adachi, K.; Ishida, Y. *Polym. J.* **1978**, *10*, 161.
- (20) Adachi, K.; Kotaka, T. *Polym. J.* **1982**, *14*, 959.
- (21) Kogowski, G. J.; Filisko, F. E. *Macromolecules*, in press.
- (22) Kogowski, G. J.; Robertson, R. E.; Filisko, F. E., to be published.
- (23) Oels, H. J.; Rehage, G. *Macromolecules* **1977**, *10*, 1036.
- (24) Rehage, G. *Ber. Bunsenges. Phys. Chem.* **1970**, *74*, 796.
- (25) Fillers, R. W.; Tschoegl, N. W. *Trans. Soc. Rheol.* **1977**, *21*, 51.
- (26) Moonan, W. K.; Tschoegl, N. W. *Macromolecules* **1983**, *16*, 55.
- (27) Cogswell, F. N.; McGowan, J. C. *Br. Polym. J.* **1972**, *4*, 183.
- (28) Plazek, D. J. *J. Phys. Chem.* **1965**, *69*, 3480.
- (29) Plazek, D. J.; O'Rourke, V. M. *J. Polym. Sci., Part A-2* **1971**, *9*, 209.
- (30) Plazek, D. J. *Polym. J.* **1980**, *12*, 43.

Theoretical Study of the Influence of the Molecular Weight on the Maximum Tensile Strength of Polymer Fibers

Yves Termonia,* Paul Meakin, and Paul Smith

Central Research and Development Department, Experimental Station, E. I. du Pont de Nemours and Company, Inc., Wilmington, Delaware 19898. Received March 9, 1985

ABSTRACT: A stochastic Monte Carlo approach, based on the kinetic theory of fracture, has been used to study the axial maximum tensile strength of polymer fibers. The approach is entirely microscopic and the inhomogeneous distribution of the external stress among atomic bonds near the chain ends is explicitly taken into account. Both primary and secondary bonds are assumed to break during fracture of the polymer fiber. The approach has been applied to perfectly oriented and ordered polyethylene fibers, for which approximate values of the model's parameters were obtained from experiment. Stress-strain curves have been calculated for several fibers of various (monodisperse) molecular weights and predictions for the tensile strength have been compared to experimental values.

1. Introduction

Values of the maximum tensile modulus have been measured or calculated for many polymers¹ and have proven to be very useful in setting goals for polymer materials research.²⁻⁴ The maximum tensile strength of polymers is a less satisfying issue. Some authors, with widely different results, have addressed the theoretical ultimate breaking stress of single chains.⁵⁻⁷ Such treatments, however, are only of value for hypothetical specimens comprising infinitely long chain molecules and are not necessarily relevant for finite molecular weights. Experimental tensile strength data, obtained for drawn fibers, have been extrapolated to infinitely small fiber diameter⁸ and this procedure has led sometimes to agreement with some of the above-mentioned values for the breaking stress of a single chain. Some attempts have been made to describe the development of tensile strength with draw ratio^{9,10} and purely empirical extrapolations of the tensile strength to the theoretical modulus have also been reported.^{11,12} Despite various theoretical and some empirical efforts, no relation for relatively simple issues such as the effect of the molecular weight on the maximum tensile strength has appeared in the polymer literature, other than Flory's expression¹³ for the tensile strength of cross-linked isotropic rubbers. All in all, the maximum tensile strength of polymeric materials of finite molecular weight and the relation to the ultimate breaking stress of infinitely long chains remains an obscure, ill-understood topic.

A theoretical study of the tensile strength of polymer fibers is an extremely complex problem. Many structural parameters, such as amorphous defects, trapped entanglements, chain ends, misalignment, etc., need to be considered. In fact, a detailed knowledge of the fiber structure is required on a molecular level. But, even in the presence of such information, a theoretical treatment of the tensile properties remains an enormous task. For that reason, all previous theories have made many simplifying assumptions

with regard to the structure and the failure mechanism. For example, classical continuum mechanics, e.g., Griffith-type approaches,¹⁴ fail to take into account the inhomogeneous nature of the structures of interest. Kinetic theories of fracture commonly focus on only one mode of failure, i.e., merely primary bond breakage,^{15,16} or pure slippage,^{17,18} while both mechanisms are known to operate during fracture of polymer fibers.¹⁹ Other kinetic theories²⁰ ignore the important contributions of the intermolecular interactions altogether.

Due to the complexity of a general theoretical treatment of the strength of polymer fibers, the present study is restricted to the case of ideal fibers made of a perfectly ordered array of fully extended macromolecules, with no defects other than chain ends resulting from finite molecular weight. As such, the study deals with the maximum axial tensile strength, which is of obvious interest, much like the knowledge of the theoretical modulus has proven to be. The present approach, which is based on the kinetic theory of fracture, is entirely microscopic and the inhomogeneous distribution of the external stress among atomic bonds near the chain ends is explicitly taken into account. The bonds are viewed as coupled oscillators in a state of constant thermal vibration. The basic events are controlled by thermally activated bond breakage and the accumulation of those events leads to crack formation and, ultimately, to the breakdown of the fiber. The bond breakages are simulated by a Monte Carlo process on a three-dimensional array of nodes, representing the elementary repetition unit of a polymer. These nodes are joined in the *x* and *z* directions by weak secondary bonds, e.g., hydrogen or van der Waals forces, whereas in the *y* direction, stronger bonds account for the primary (C-C) forces. Our model thus resembles that of Dobrodumov and El'yashevitch²¹ except for the fact that, in the latter, it was assumed that only primary bonds can break. Here, in contrast, we allow fiber fracture to proceed by the breaking